Volume 46 | Number 42 | 14 November 2017 | Pages 14423–14702

Dalton Transactions

An international journal of inorganic chemistry

rsc.li/dalton

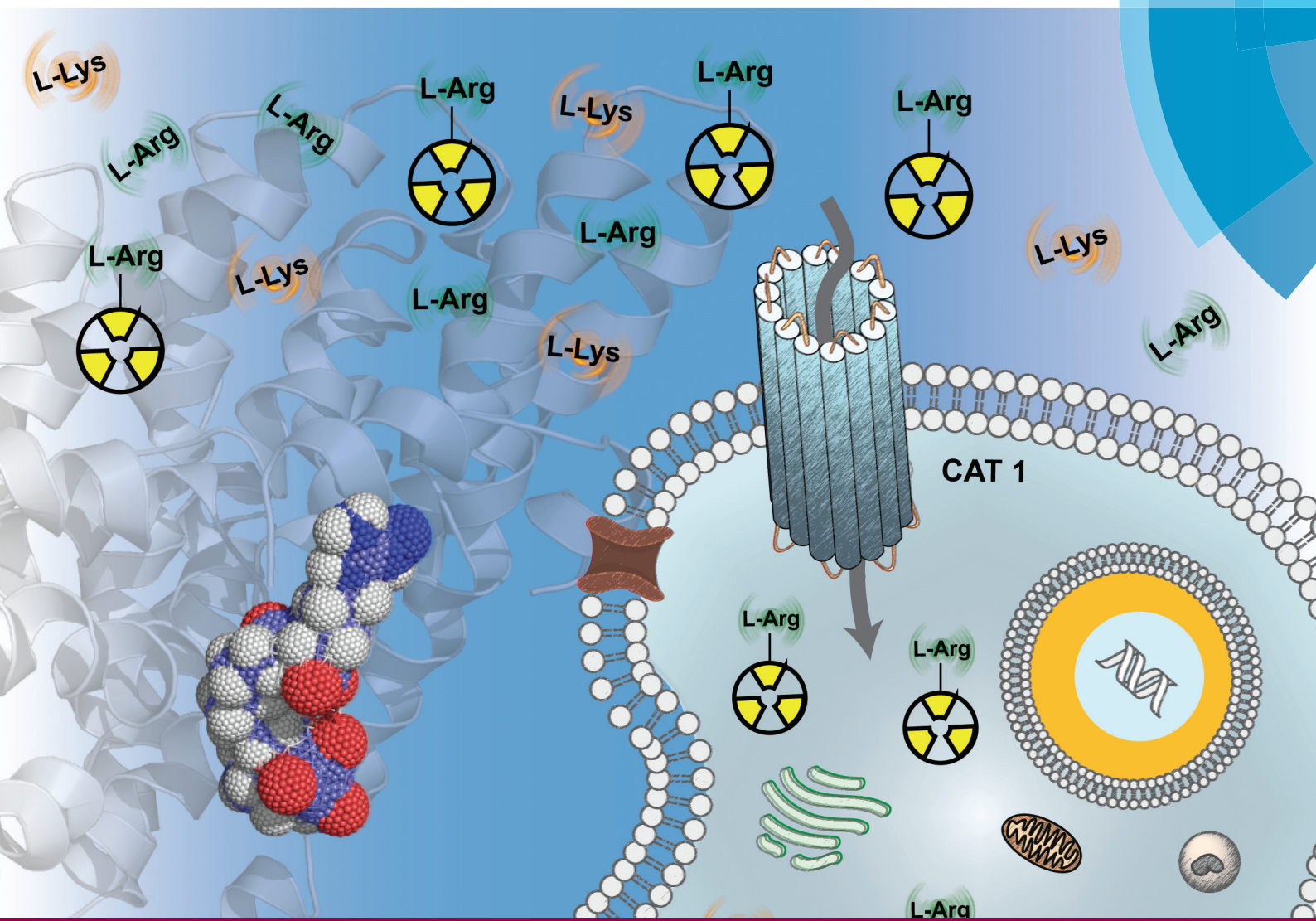

Themed issue: Frontiers in Radionuclide Imaging and Therapy

ISSN 1477-9226

ROYAL SOCIETY OF CHEMISTRY

PAPER

João D. G. Correia *et al.*

Technetium-99m complexes of L-arginine derivatives for targeting amino acid transporters

Dalton Transactions

PAPER

View Article Online
View Journal | View Issue

Cite this: *Dalton Trans.*, 2017, **46**, 14537

Technetium-99m complexes of L-arginine derivatives for targeting amino acid transporters†

Maurício Morais, ‡§ Vera F. C. Ferreira, § Flávio Figueira, Filipa Mendes, Paula Raposinho, Isabel Santos, Bruno L. Oliveira ¶ and João D. G. Correia *

Although relevant from the clinical point of view, radiotracers targeting cationic amino acid transporters are relatively unexplored and, in particular, no metal-based radiotracers are known. The rare examples of complexes recognized by amino acid transporters, namely by the Na^+-independent neutral L-type amino acid transporter 1 (LAT1), are $^{99m}Tc(I)/Re(I)$ compounds. Herein, we describe conjugates comprising a pyrazolyl-diamine chelating unit and the cationic amino acid L-arginine (L-Arg) linked by a propyl (**L^1**) or hexyl linker (**L^2**), which allowed the preparation of stable complexes of the type *fac*-$[^{99m}Tc(CO)_3(k^3\text{-L})]^+$ (**Tc1**, L = **L^1**; **Tc2**, L = **L^2**) and of the respective surrogates **Re1** and **Re2**. Interestingly, complex **Tc2** exhibited moderate levels of time-dependent internalization in three human tumoural cell lines, with approximately 3% of total applied activity internalized, corresponding to 21% of the cell-associated activity. A putative mechanism of retention in the cytoplasm of cells could be the interaction of the complex with inducible nitric oxide synthase (iNOS), which is the enzyme responsible for the catalytic oxidation of L-Arg to citrulline and nitric oxide. However, the surrogate complex **Re2** does not recognize iNOS, as demonstrated by the *in vitro* assays with purified iNOS and in studies with lipopolysaccharide(LPS)-activated macrophages. Preliminary mechanistic studies suggest that the internalization of **Tc2** is linked to the cationic amino acid transporters, namely system y^+. This finding might open the way towards the development of novel families of metal-based radiotracers for probing metabolically active cancer cells.

Received 30th March 2017,
Accepted 30th May 2017

DOI: 10.1039/c7dt01146f

rsc.li/dalton

Introduction

The majority of the Positron Emission Tomography (PET) imaging procedures rely on the use of the glucose analogue 2-[^{18}F]fluoro-2-deoxy-D-glucose ([^{18}F]FDG), which enters the cells *via* membrane glucose transporters, where it undergoes phosphorylation and is irreversibly trapped.[1,2] Accumulation of this radiopharmaceutical in tumoural cells is mainly due to the upregulation of glucose transport and glycolysis. However, [^{18}F]FDG presents some limitations, including limited visualization of brain tumors, low or variable uptake in some tumor types (*e.g.* prostate cancer and neuroendocrine tumors) and increased accumulation in inflammatory lesions.[3,4] Thus, radiolabeled amino acids, which target increased rates of amino acid transport in cancer cells, have been considered as alternatives to overcome some of these limitations.[5,6] Indeed, they are accepted as tracers for imaging the upregulated metabolism linked to several hallmarks of cancer.

The transport of amino acids across the plasma membrane into the cytoplasm of mammalian cells is mediated by membrane-bound transport systems that present varying substrate specificities, pH and sodium dependence, and regulatory mechanisms.[6–8] Most of the studies performed so far have been based on radiolabeled amino acids for targeting the "L amino acid transport system", which preferentially transports amino acids with neutral side chains like L-Leu, L-Tyr, and L-Phe.[9,10] Relevant tracers from this class include L-^{11}C-methionine and *O*-(2-^{18}F-fluoroethyl)-L-tyrosine (^{18}F-FET) for imaging brain tumors, and 6-^{18}F-fluoro-3,4-dihydroxy-L-phenylalanine (^{18}F-FDOPA) for imaging neuroendocrine tumors. In the past few years there has been growing interest in the design of tracers for targeting other amino acid transporters, including "system A", glutamine, glutamate and cationic amino acid transporters.[9] The transport of basic amino acids (L-Lys, L-Arg and L-His) is mediated by sodium-independent

Centro de Ciências e Tecnologias Nucleares, Instituto Superior Técnico, Universidade de Lisboa, Estrada Nacional 10 (km 139.7), 2695-066 Bobadela LRS, Portugal. E-mail: jgalamba@ctn.tecnico.ulisboa.pt; Tel: +351 21 994 62 33

†Electronic supplementary information (ESI) available. See DOI: 10.1039/c7dt01146f

‡Current address: Division of Imaging Sciences and Biomedical Engineering, King's College London, 4th Floor Lambeth Wing, St Thomas' Hospital, London SE1 7EH, United Kingdom.

§These authors contributed equally to the article.

¶Current address: Department of Chemistry, University of Cambridge, Lensfield Road, Cambridge, United Kingdom.

and sodium-dependent transporter systems, which include the cationic amino acid transporter (CAT, system y^+) family, system y^+L, $b^{0,+}AT$ and $ATB^{0,+}$.

The amino acid L-Arg is the precursor for relevant metabolic pathways such as agmatine, creatine, urea, and nitric oxide (NO) synthesis.[11] The latter is a mammalian signaling molecule biosynthesized by NO synthases (NOS) with high relevance in physiological (*e.g.* neuronal transmission) and pathological processes (*e.g.* cancer and neurological disorders).[12–14] Additionally, L-Arg is a relevant signaling molecule that regulates essential cellular functions such as protein synthesis, apoptosis and growth.[11] It also plays an important role in cells lacking argininosuccinate synthase 1 (ASS1), one of the key urea cycle enzymes that is absent in many tumors, suggesting that tumoral ASS1 deficiency may be both a prognostic biomarker and predictor of sensitivity to arginine deprivation therapy.[15] Brought together the pathophysiological roles of L-Arg and the fact that certain cancer cells overexpress cationic amino acid transporters such as $ATB^{0,+}$ or CAT1,[16–20] indicate that radiolabelled L-Arg derivatives hold potential for cancer imaging. Moreover, radiolabelled L-Arg derivatives could be envisaged as imaging biomarkers for predicting and monitoring response to arginine deprivation therapy.

Although potentially relevant from the clinical point of view, radiotracers targeting cationic amino acid transporters are relatively unexplored and, in particular, no metal-based radiotracers are known.[6,9] So far, the only examples of metal complexes recognized by amino acid transporters and actively internalized into cancer cells, more specifically through the L-type LAT1, have been ^{99m}Tc(I)/Re(I) complexes.[21] One of the main advantages of using ^{99m}Tc-based complexes, compared to using cyclotron-produced radionuclides such as ^{11}C or ^{18}F, relies on the fact that ^{99m}Tc is easily available in nuclear medicine centres worldwide through ^{99}Mo/^{99m}Tc generators. Moreover, it is considered to burden a low dose of radiation to patients. Considering our previous work in the design and biological evaluation of novel Tc(I)/Re(I) complexes with pendant L-Arg derivatives for visualization of NO/NOS-related tumors by SPECT imaging,[22–26] we describe herein the (radio)synthesis, biological evaluation and preliminary mechanistic studies of novel ^{99m}Tc(I)-labelled L-Arg derivatives useful for imaging metabolically active cells.

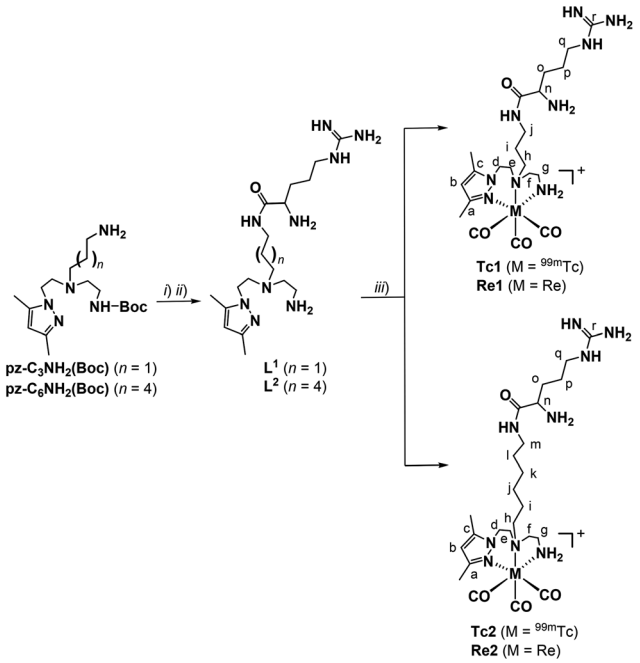

Scheme 1 Synthesis of $\mathbf{L^1}$, $\mathbf{L^2}$, **Tc1/Re1** and **Tc2/Re2** (identification system for NMR assignments is displayed for the rhenium complexes). (i) Et_3N, *N*-α-Boc-L-Arg, HBTU, 2 h, r.t.; (ii) CH_2Cl_2–TFA, 3 h, r.t.; (iii) $[M(CO)_3(H_2O)_3]^+$ (M = Re, ^{99m}Tc), H_2O, 100 °C.

Results and discussion

Complexes of the type *fac*-$[M(CO)_3(k^3\text{-}L)]^+$ (M = Re/^{99m}Tc, L = L^1 and L^2)

We have prepared and fully characterized conjugates $\mathbf{L^1}$ and $\mathbf{L^2}$ containing L-Arg following previously described procedures.[22] Besides the pendant amino acid moiety, the conjugates present a pyrazolyl-diamine chelating unit known to stabilize efficiently the organometallic core *fac*-$[M(CO)_3]^+$ (M = ^{99m}Tc or Re), which already allowed the radiolabeling of various molecules with biological relevance.[23,27] In brief, the conjugates were prepared upon conjugation of the Boc-protected precursors **Pz-C$_3$NH$_2$(Boc)** and **Pz-C$_6$NH$_2$(Boc)** to *N*-α-Boc-L-Arg (Scheme 1), respectively, using standard coupling reagents and conditions (HBTU, Et_3N, 2 h, room temperature), followed by hydrolysis of the protecting groups with trifluoroacetic acid (TFA).

Conjugates $\mathbf{L^1}$ and $\mathbf{L^2}$ were obtained in high purity (≥98% ascertained by RP-HPLC, Fig. S1†) as stable colorless oils after purification by semi-preparative reversed phase high performance liquid chromatography (RP-HPLC). The conjugates were fully characterized by ^{1}H/^{13}C NMR (Fig. S2 and S3†) and IR spectroscopy as well as electrospray ionization mass spectrometry.

The radioactive complexes *fac*-$[^{99m}Tc(CO)_3(k^3\text{-}L)]^+$ (**Tc1**, L = $\mathbf{L^1}$; **Tc2**, L = $\mathbf{L^2}$, Scheme 1) were prepared in high radiochemical yield and radiochemical purity (>95%) upon reaction of $\mathbf{L^1}$ or $\mathbf{L^2}$ with the precursor *fac*-$[^{99m}Tc(CO)_3(H_2O)_3]^+$ (Fig. S4†). The latter was prepared by addition of Na[$^{99m}TcO_4$], eluted from a ^{99}Mo/^{99m}Tc generator with saline solution, to an IsoLink kit (Mallinckrodt, Covidien) available for research purposes, and heating (95 °C) for 20 min. The high stability of the resulting final complexes was demonstrated by incubation with a 100-fold excess of coordinating amino acids such as histidine (Fig. S5†) or cysteine. No relevant degradation or transchelation was detected by RP-HPLC after incubation at 37 °C for up to 6 h in line with earlier results obtained for complexes stabilized by the same chelating unit.[22,27,28] Additional stability studies demonstrated that the complexes are also stable in human plasma.

The dilute nature of solutions of ^{99m}Tc complexes (*ca.* 10^{-9}–10^{-12} M) hampers their structural characterization by the

usual analytical methods in chemistry. The more straightforward way to overcome this limitation is to compare the chromatographic behavior of ^{99m}Tc complexes with that of the surrogate rhenium complexes prepared at the "macroscopic" scale, since technetium and rhenium, transition metals of group 7 of the periodic table share similar coordination chemistry. Thus, the chemical identity of **Tc1** and **Tc2** was confirmed by comparing their RP-HPLC radioactive traces (γ detection) with the UV-Vis traces of the surrogate complexes **Re1** and **Re2** (Fig. S6†). These complexes were synthesized upon reaction of $\mathbf{L^1}$ and $\mathbf{L^2}$ with *fac*-$[Re(CO)_3(H_2O)_3]^+$ in refluxing water (Scheme 1), and were obtained in moderate yields (35–75%) after purification by semi-preparative RP-HPLC.

Re1 and **Re2** were fully characterized by ESI-MS, IR and ^{1}H/^{13}C NMR spectroscopy. The data collected support the proposed structure and the tridentate coordination mode of the pyrazolyl-diamine chelating unit, comparing well with similar complexes previously described by our group.[22,27,29]

Cellular uptake studies

Aimed at predicting the *in vivo* tumor-targeting properties of **Tc1** and **Tc2** and to assess their ability to be recognized and internalized as specific substrates by the transporters of L-Arg, we have performed uptake studies in a panel of human tumoral cell lines, more specifically HeLa cervical cancer, A375 melanoma, MDA-MB-231 breast cancer and PC3 prostate cancer cell lines. The results of the cellular uptake as a function of the incubation time are presented in Fig. 1.

Complex **Tc2** displayed a remarkably higher uptake than **Tc1**, with values between 11.4 ± 0.7% (HeLa cell line) and 15.1 ± 0.3% (A375 cell line) after 3 h incubation. We speculate that the difference observed between the uptake values for the two radioconjugates might be assigned to the presence of a longer alkyl chain in **Tc2** (hexyl linker) than in **Tc1** (propyl linker), assuming that these arginine derivatives are substrates of the Na^+-independent transport system y^+, which has been postulated to be the major entry route for cationic amino acids, L-Arg included, in most cells.

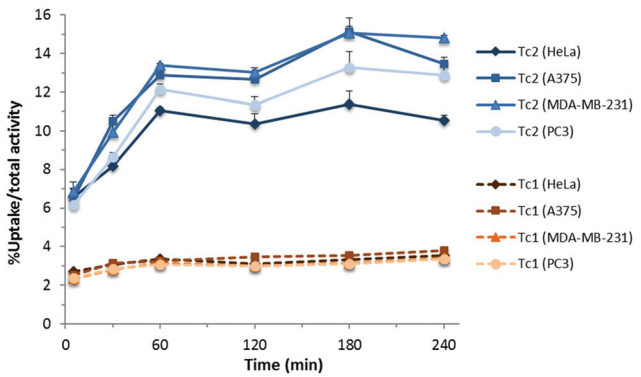

Fig. 1 Cellular uptake of **Tc1** and **Tc2** in human cancer cell lines at 37 °C.

Indeed, it has been reported that for system y^+, CAT proteins have a higher affinity towards cationic amino acids with a longer carbon backbone: homoarginine > arginine > lysine > ornithine > 2,4-diamino-*n*-butyric acid.[8] Another clue suggesting the involvement of the system y^+ in the cellular uptake of **Tc1** and **Tc2** is the fact that analogue radioconjugates with pendant N^{ω}-NO_2-L-arginine moieties (**Tc3–Tc5**, Scheme 2), previously prepared for targeting NOS,[22,28] are not taken up by the cell lines tested (Fig. 2).

In fact, it has been described that the inhibitors of NOS such as N^{ω}-NO_2-L-arginine methyl ester or *N*-methyl arginine competitively inhibit arginine transport across cell membranes due to interaction with system y^+.[30]

The remarkable cellular uptake results obtained with **Tc2** prompted us to deepen these studies in an attempt to unveil the most likely cellular uptake mechanism, using both the radioactive complex **Tc2** and the "cold" surrogate **Re2**. Therefore, internalization studies in HeLa, A375 and MDA-MB-231 cancer cell lines have been performed, and the results are displayed in Fig. 3A.

Tc2 exhibits moderate levels of time-dependent internalization with the highest values being reached at 4 h in all cell lines: 2.7 ± 0.2% (A375), 3.0 ± 0.3% (MDA-MB-231) and 3.2 ± 0.3% (HeLa) of the total applied activity internalized, corresponding to 21.3 ± 0.8%, 21.6 ± 1.3% and 22.5 ± 1.0% of the cell-associated activity, respectively.

Aimed at clarifying the role of the transporters of cationic amino acids in the uptake and internalization of **Tc2**, and considering that L-Lys competes with L-Arg for common transport systems,[11,31,32] we have performed internalization studies of **Tc2** with co-incubation with L-Lys in the same cell lines (Fig. 3B). Although moderate, the inhibition of cell surface-bound **Tc2** (17%, 25% and 18% for HeLa, MDA-MB-231 and A375 cell lines, respectively) and, more importantly, the inhibition of internalized **Tc2** (20%, 29% and 36%, respectively) suggest the involvement of the transporters of cationic amino acids in the cell uptake mechanism of **Tc2**.

Furthermore, we have also studied the contribution of the CAT family (system y^+), more specifically of CAT1, upregulated in various cancers,[19,20] in the specific uptake of **Tc2**. Firstly, we have confirmed the expression of CAT1 in the selected cell lines by western blot analysis of protein extracts using an anti-CAT1 antibody (Fig. 4).

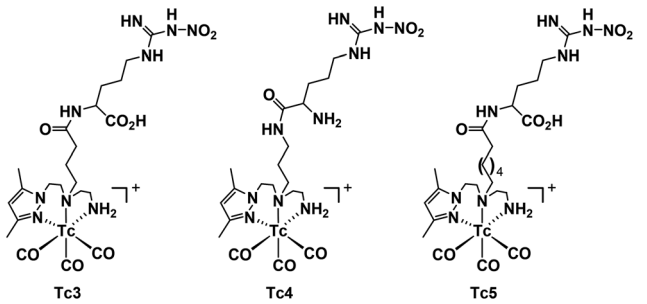

Scheme 2 Molecular structures of **Tc3–Tc5**.

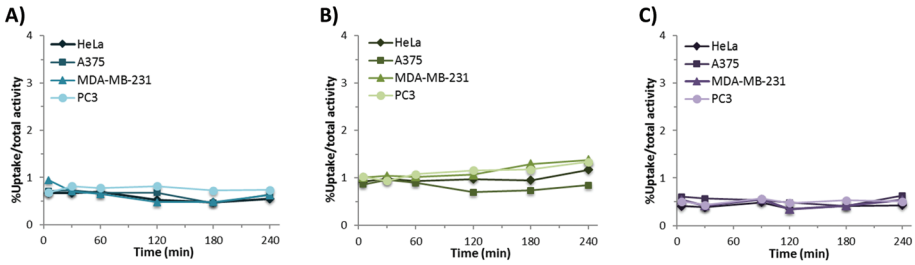

Fig. 2 Cellular uptake of the radioconjugates **Tc3** (A), **Tc4** (B) and **Tc5** (C) in various human cancer cell lines at 37 °C.

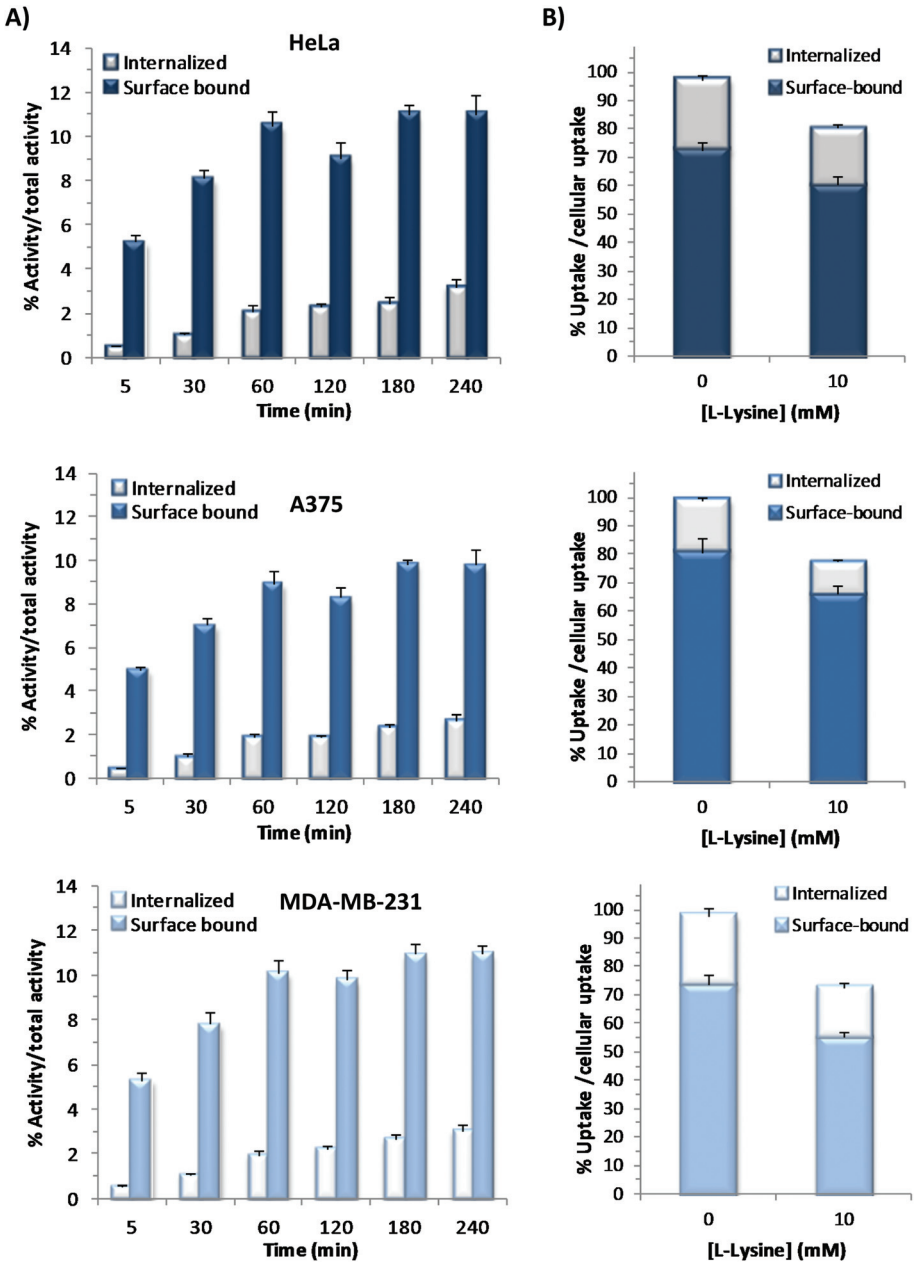

Fig. 3 (A) Internalized and surface-bound **Tc2** in HeLa, A375 and MDA-MB-231 cancer cell lines at 37 °C, expressed as a percentage of the total applied activity. (B) Internalized and surface-bound **Tc2** after 2 h in the presence of lysine at 37 °C, expressed as a percentage of cellular uptake in the absence of L-Lys.

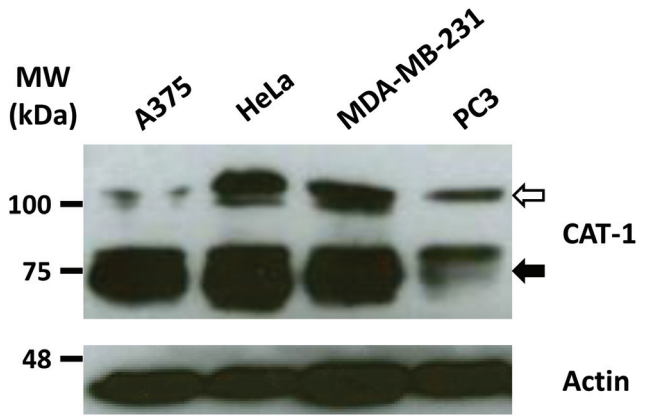

Fig. 4 Evaluation of CAT1 expression in HeLa cervical cancer, A375 melanoma, MDA-MB-231 breast cancer and PC3 prostate cancer cell lines. Bands corresponding to the unglycosylated (*ca.* 70 kDa) form and glycosylated form (*ca.* 90 kDa) of CAT1 are observed. Actin was used as an internal loading control.

Then, we performed cell uptake assays in the presence of the cysteine-modifying agent *N*-ethylmaleimide (NEM), which has been recently shown to inhibit selectively all human CATs (system y^+), but no other transporters of cationic amino acid transporters such as the y^+LAT isoform.[33] The results of the cell uptake studies are presented in Fig. 5.

Under the conditions tested, the cellular uptake of **Tc2** is inhibited by NEM in 10.5%–20.9% after 5 to 60 minutes incubation (Fig. 5B), which supports our hypothesis of CAT1-mediated internalization of this complex.

Although the results presented above may suggest that the sodium-independent transporter CAT1 is implicated in the transport of **Tc2** across cell membranes, the contribution of sodium-dependent transporters such as amino acid transport systems $b^{0,+}$AT and $ATB^{0,+}$ cannot be discarded at this point.

The driving force for **Tc2** internalization could also be strengthened by the simultaneous contribution of a specific mechanism of retention in the cytosol of the cell, namely by interaction of the complex with cytosolic NOS, which we have already demonstrated to be the case for complexes of a related family mentioned above.[22] To test this hypothesis we have studied the ability of **Re1** and **Re2**, cold surrogates of **Tc1** and **Tc2**, to be recognized by NOS both in enzymatic assays with purified iNOS and in LPS-activated macrophages. For the sake of comparison, the corresponding ligands **L1** and **L2** were also tested.

Firstly, the molecules were tested as NO-producing substrates using mouse recombinant iNOS. The iNOS activity was determined spectrophotometrically by monitoring the NO-mediated conversion of oxyhemoglobin to methemoglobin at 401 nm and 421 nm as previously described.[22,29] Table 1 displays the kinetic parameter K_m for all compounds, which was determined by the method of Eisenthal and Cornish-Bowden.

The ability of **L1** (K_m = 50 μM) to interact specifically with the active site of iNOS, leading to NO production, is considerably higher than that observed for **L2** (K_m = 1200 μM); however, both compounds are poorer substrates than the endogenous substrate (L-Arg) of the enzyme (K_m = 3 μM). Metallation of **L1** and **L2** led to complexes with even lower NO-producing properties, as evidenced by the determined K_m values (**Re1**, K_m = 1093 μM; **Re2**, K_m > 2500 μM).

The effect of the same compounds was also studied in RAW 264.7 macrophages after treatment with lipopolysaccharide (LPS), which leads to increased NO biosynthesis due to iNOS

Table 1 K_m values for L-Arg, **L1**, **L2**, **Re1** and **Re2**

Compound	K_m values/μM
L-Arg	3.00 ± 1.00
L1	50
Re1	1093
L2	1200
Re2	>2500

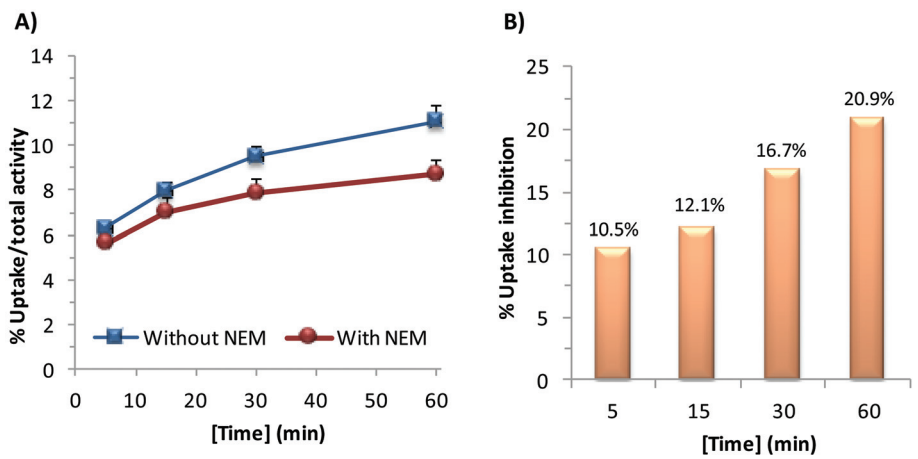

Fig. 5 (A) Cellular uptake of **Tc2** in the A375 melanoma cell line at different time points at 37 °C in the presence of *N*-ethylmaleimide (NEM, 5 mM). (B) Inhibition of cellular uptake by NEM expressed in percentage.

overexpression.[22,34] This cellular model is very useful, as it allows one to assess both the capacity of the compounds to cross cellular membranes, a key feature for improving tracer uptake *in vivo*, and the intracellular interaction with the iNOS enzyme *via* the quantitation of the NO release.

The results, which represent the ability of the compounds to be recognized and used as NOS substrates and, consequently, their efficacy in NO biosynthesis in LPS-activated macrophages cultured in arginine-free medium, are presented in Fig. 6.

When LPS-induced macrophages were incubated in L-Arg-free culture medium, negligible NO production was observed. However, when macrophages were incubated with various concentrations of L-Arg (100–700 μM) a high nitrite accumulation in the extracellular medium was observed (data not shown).

Incubation of LPS-treated macrophages with the new compounds showed that $\mathbf{L^1}$ and $\mathbf{L^2}$ are recognized as substrates by the enzyme, confirmed by NO production (*ca.* 50%). When the corresponding rhenium compounds **Re1** and **Re2** are incubated with the cells the production of NO was negligible. These results are consistent with those obtained in the enzymatic assays, where it has been possible to conclude that metallation of conjugates **L1** and **L2** led to decreased affinities towards the enzyme.

We also performed a parallel viability assay to assess the intrinsic cytotoxicity of the compounds at the concentration used in the NO assay. The compounds were tested in the absence or presence of L-Arg (Fig. 7) in order to evaluate whether the viability is related with the presence/absence of NO, a key signaling mediator in several metabolic processes.

In the case of $\mathbf{L^1}$ and $\mathbf{L^2}$ the viability is similar under both conditions (approximately 100%). For metal complexes **Re1** and **Re2**, which are not utilized as substrates, the viability is decreased in the absence of L-Arg (*ca.* 50%), most likely determined by impaired NO biosynthesis, with a value comparable to the control performed in the absence of that amino acid (*ca.* 50%). However, the viability of the metal complexes is comparable to the control when that amino acid is present in the culture medium, showing that the compounds by themselves are not toxic at the concentrations tested. Altogether, these results indicated that viability was being determined by NO biosynthesis.

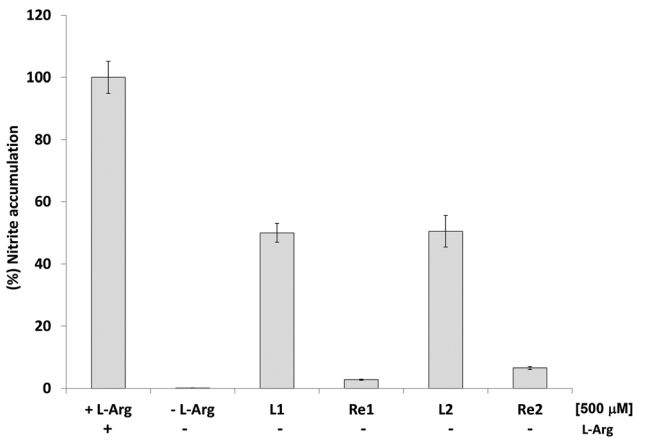

Fig. 6 Effect of **L1**, **L2**, **Re1** and **Re2** on NO biosynthesis by LPS-induced RAW 264.7 macrophages. Data are expressed as % of nitrite accumulation of the L-Arg control (mean ± S.D. – standard deviation, n = 8). The experiment was repeated three times with comparable results.

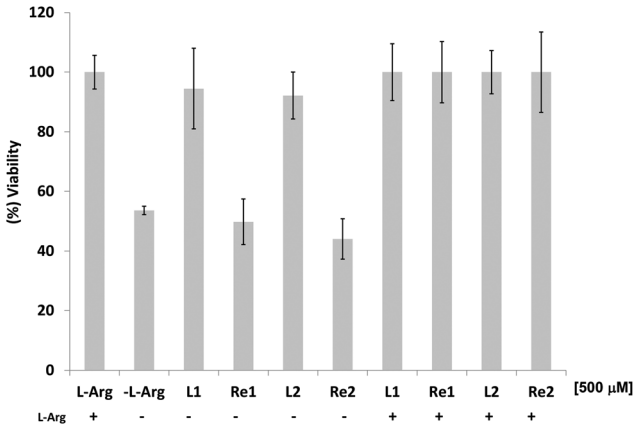

Fig. 7 Viability in macrophages RAW 264.7 incubated with the compounds, in the absence or presence of L-arginine in the culture medium. Viability of cells incubated with LPS and L-arginine was considered as 100% (mean ± S.D., n = 8). This experiment was repeated two/three times with comparable results.

Conclusions

We have prepared and characterized new conjugates comprising a pyrazolyl-diamine chelating unit and a pendant L-Arg moiety linked by a propyl ($\mathbf{L^1}$) or a hexyl linker ($\mathbf{L^2}$). The conjugates reacted with the organometallic precursors *fac*-$[M(CO)_3(H_2O)_3]^+$ (M = ^{99m}Tc/Re) yielding the radioactive complexes of the type *fac*-$[^{99m}Tc(CO)_3(k^3\text{-L})]^+$ (**Tc1**, L = $\mathbf{L^1}$; **Tc2**, L = $\mathbf{L^2}$) and the respective "cold" surrogates **Re1** and **Re2**. **Tc2** exhibited moderate levels of time-dependent internalization in three different human tumoral cell models, with about 3% of the applied activity internalized after 4 h at 37 °C, corresponding to 21% of the total cell-associated activity. Preliminary mechanistic studies suggest that internalization of **Tc2** is mediated by cationic amino acid transporters, namely system y^+, although more extensive amino acid transport assays will be needed to fully address this issue in the cancer lines studied. In addition, enzymatic assays with purified iNOS and studies with LPS-activated macrophages demonstrate that the surrogate complex **Re2** does not recognize a putative target of **Tc2** in the cytosol. Nevertheless, **Tc2** is a rare example of a metal complex whose entrance into cells seems to be mediated by cationic amino acid transporters. This finding might open the way towards the development of novel families of metal-based radiotracers to probe metabolically active cancer cells.

Experimental section

General procedures and materials

All chemicals and solvents were of reagent grade and were used without purification unless stated otherwise. The BOC-protected precursors *tert*-butyl 2-((3-aminopropyl)(2-(3,5-dimethyl-1*H*-pyrazol-1-yl)ethyl)amino)ethylcarbamate (**Pz-C$_3$NH$_2$(Boc)**), *tert*-butyl 2-((6-aminohexyl)(2-(3,5-dimethyl-1*H*-pyrazol-1-yl)ethyl)amino)ethylcarbamate (**Pz-C$_6$NH$_2$(Boc)**), and [Re(CO)$_3$(H$_2$O)$_3$]Br were prepared according to published methods.[22,35] 2-(*tert*-Butoxycarbonylamino)-5-guanidinopentanoic acid (*N*-α-Boc-L-Arg) was purchased from Sigma Aldrich as well as all other chemicals not specified above. Na[^{99m}TcO$_4$] was eluted from a ^{99}Mo/^{99m}Tc generator, using 0.9% saline. The radioactive precursor *fac*-[^{99m}Tc(CO)$_3$(H$_2$O)$_3$]$^+$ was prepared using an IsoLink® kit (Covidean Malinckrodt, Inc.). ^{1}H and ^{13}C NMR spectra were recorded at room temperature on a Varian Unity 300 MHz spectrometer. ^{1}H and ^{13}C chemical shifts were referenced with the residual solvent resonances relatively to tetramethylsilane. The spectra were assigned with the help of 2D experiments (^{1}H–^{1}H correlation spectroscopy, COSY and ^{1}H–^{13}C heteronuclear single quantum coherence, HSQC). Assignments of the ^{1}H and ^{13}C NMR resonances are given in accordance with the identification system shown in Scheme 1. Infrared spectra were recorded as KBr pellets on a Bruker Tensor 27 spectrometer. All compounds were characterized by electrospray ionization mass spectrometry (ESI-MS) using a Bruker model Esquire 3000 plus. HPLC analyses were performed on a PerkinElmer LC pump 200 coupled to a Shimadzu SPD 10AV UV/Vis and to a Berthold-LB 509 radiometric detector, using an analytic Macherey-Nagel C18 reversed-phase column (Nucleosil 100-5, 250 × 3 mm) with a flow rate of 0.5 mL min^{-1}. Eluents: aqueous 0.1% CF_3CO_2H/MeOH. Gradient: t = 0–5 min: 10% MeOH; 5–30 min: 10 → 100% MeOH; 30–34 min: 100% MeOH; 34–35 min: 100 → 10% MeOH; 35–40 min: 10% MeOH.

Purification of the inactive compounds was achieved on a semi-preparative Macherey-Nagel C18 reversed-phase column (Nucleosil 100-7, 250 × 8 mm) or on a preparative Waters μBondapak C18 (150 × 19 mm) with a flow rate of 2.0 mL min^{-1} and 5.5 mL min^{-1}, respectively. UV detection: 220 or 254 nm. Eluents: aqueous 0.1% CF_3CO_2H/MeOH. Gradient: t = 0–5 min: 10% MeOH; 5–30 min: 10 → 100% MeOH; 30–34 min: 100% MeOH; 34–35 min: 100 → 10% MeOH; 35–40 min: 10% MeOH.

Aliquots of ~5 mg of pure compounds (≥98% ascertained by RP-HPLC) were lyophilized in microcentrifuge tubes and used for radioactive labelling and *in vitro* studies.

Synthesis of *tert*-butyl 2-((3-(2-amino-5-guanidinopentanamido)propyl)(2-(3,5-dimethyl-1*H*-pyrazol-1-yl)ethyl)amino)ethylcarbamate (L^1-Boc)

To a solution of **Pz-C$_3$NH$_2$(Boc)** (0.050 g, 0.140 mmol) in dimethylformamide (DMF) were added triethylamine (0.036 g, 0.365 mmol) and *O*-benzotriazol-1-yl-*N*,*N*,*N*′,*N*′-tetramethyluronium hexafluorophosphate (HBTU, 0.054 g, 0.145 mmol). After 10 min, *N*-α-Boc-L-Arg (0.039 g, 0.142 mmol) was added, and the reaction mixture was stirred at room temperature under a nitrogen atmosphere for 2 h. The solvent was removed under vacuum, and the residue was purified by silica gel column chromatography using a gradient of MeOH (0 → 100%) in $CHCl_3$. The intermediate **L^1-Boc** was obtained as a yellowish oil. Yield: 58.1% (0.050 g, 0.082 mmol).

^{1}H-NMR (300 MHz, $CDCl_3$): δ_H (ppm) 7.69 (2H, br s, NH), 6.48 (1H, br s, NH), 5.70 (1H, s, CH^b), 5.10 (1H, br s, NH), 5.01 (2H, t, CH$_2^d$), 4.57 (1H, br s, NH), 3.35 (2H, t, CH$_2^e$), 3.07 (1H, br m, CH^k), 2.86–2.80 (4H, m, CH$_2^{g, j}$), 2.35 (2H, t, CH$_2^n$), 2.32 (2H, t, CH$_2^f$), 2.23 (2H, t, CH$_2^g$), 2.19 (3H, s, CH$_3^{Pz}$), 2.16 (3H, s, CH$_3^{Pz}$), 1.40–1.38 (18H, s, CH$_3^{Boc}$), 1.39–1.15 (6H, m, CH$_2^{i, l, m}$).

^{13}C-NMR (75.5 MHz, $CDCl_3$): δ_C (ppm) 174.3 (CO), 172.6 (CO), 159.4 (C^o), 147.3 (C^{Pz}), 143.9 (C^{Pz}), 106.9 (C^{Pz}), 79.9 (C(CH$_3$)$_3$), 56.7 (C^e), 54.1 (C^k), 53.8 (C^f), 51.6 (C^h), 49.2 (C^d), 41.2 (C^n), 38.9 (C^g), 38.0 (C^j), 30.8 (C^i), 28.8 (C(CH$_3$)$_3$), 25.4 (C^l), 24.6 (C^m), 13.4 (CH$_3$Pz), 11.0 (CH$_3$Pz).

Synthesis of *tert*-butyl 2-((6-(2-amino-5-guanidinopentanamido)hexyl)(2-(3,5-dimethyl-1*H*-pyrazol-1-yl)ethyl)amino)ethylcarbamate (L^2-Boc)

To a solution of **Pz-C$_6$NH$_2$(Boc)** (0.050 g, 0.131 mmol) in DMF were added triethylamine (0.036 g, 0.365 mmol) and *O*-benzotriazol-1-yl-*N*,*N*,*N*′,*N*′-tetramethyluronium hexafluorophosphate (HBTU, 0.054 g, 0.145 mmol). After 10 minutes, *N*-α-Boc-L-Arg (0.039 g, 0.142 mmol) was added, and the reaction mixture was stirred at room temperature under a nitrogen atmosphere for 2 h. The solvent was then removed under vacuum, and the residue was purified by silica gel column chromatography using a gradient of MeOH (0 → 100%) in $CHCl_3$. The intermediate **L2-Boc** was obtained as a yellowish oil. Yield: 60.2% (0.050 g, 0.078 mmol).

^{1}H-NMR (300 MHz, $CDCl_3$): δ_H (ppm) 7.70 (2H, br s, NH), 6.51 (1H, br s, NH), 5.73 (1H, s, CH^b), 5.14 (1H, br s, NH), 5.05 (2H, t, CH$_2^d$), 4.61 (1H, br s, NH), 3.37 (2H, t, CH$_2^e$), 3.13 (1H, br m, CH^n), 3.13–3.06 (4H, m, CH$_2^{g, m}$), 2.65 (2H, t, CH$_2^h$), 2.52 (2H, t, CH$_2^q$), 2.43 (2H, t, CH$_2^f$), 2.20 (3H, s, CH$_3^{Pz}$), 2.18 (3H, s, CH$_3^{Pz}$), 1.80 (2H, q, C^o), 1.80 (2H, m, C^l), 1.42–1.40 (18H, s, CH$_3^{Boc}$), 1.32–1.26 (6H, m, CH$_2^{i, j, k}$).

^{13}C-NMR (75.5 MHz, $CDCl_3$): δ_C (ppm) 174.5 (CO), 172.8 (CO), 158.4 (C^r), 147.5 (C^{Pz}), 144.2 (C^{Pz}), 105.9 (C^{Pz}), 79.5 (C(CH$_3$)$_3$), 56.7 (C^e), 56.3 (C^h), 54.1 (C^f), 53.6 (C^n), 49.4 (C^d), 41.5 (C^q), 39.3 (C^m), 38.8 (C^g), 30.6 (C^n), 28.9 (C(CH$_3$)$_3$), 28.3 (C^i), 27.6 (C^j), 26.4 (C^k), 25.6 (C^o), 24.9 (C^p), 13.5 (CH$_3^{Pz}$), 11.3 (CH$_3^{Pz}$).

Synthesis of 2-amino-*N*-(3-((2-aminoethyl)(2-(3,5-dimethyl-1*H*-pyrazol-1-yl)ethyl)amino)-propyl)-5-guanidinopentanamide (L^1)

Compound **L^1** was obtained directly by dissolving **L^1-Boc** (0.050 g, 0.082 mmol) in a mixture CH_2Cl_2–TFA (1 mL–3 mL) and allowed to react for 3 h at room temperature with stirring. The residue obtained after evaporation of the solvents was dissolved in water, filtered through a 0.45 μm Millipore filter, and purified by preparative RP-HPLC. The fractions containing **L^1** were collected and the solvent was removed to provide a clear

viscous oil. Yield: 78% (0.026 g, 0.061 mmol, calcd for $C_{19}H_{41}N_9O$).

^{1}H-NMR (300 MHz, D_2O): δ_H (ppm) 5.99 (1H, s, H^b), 4.37 (2H, s, H^d), 3.86 (1H, t, H^n), 3.49 (2H, m, H^e), 3.39 (2H, m, H^f), 3.32 (2H, t, H^g), 3.24–3.06 (6H, t, $H^{q,\ h,\ j}$) 2.19 (3H, s, CH_3^{Pz}), 2.10 (3H, s, CH_3^{Pz}), 1.81 (4H, m, $H^{o,\ i}$), 1.53 (2H, m, H^p).

^{13}C-NMR (75.5 MHz, D_2O): δ_C (ppm) 169.9 (CO), 156.9 (C^r), 148.9 (C^c), 144.4 (C^a), 107.3 (C^b), 52.9 (C^n), 51.8 (C^h), 51.7 (C^e) 49.9 (C^f), 42.2 (C^d), 40.4 (C^q), 36.4 (C^j), 33.9 (C^g), 28.1 (C^i), 23.8 (C^o), 23.4 (C^p), 11.5 (CH_3^{Pz}), 10.1(CH_3^{Pz}).

RP-HPLC (t_R): 18.7 min.

ESI-MS (+) (m/z): 412.7 $[M + H]^+$, calcd for $C_{19}H_{41}N_9O$ = 411.6.

IR (KBr, cm^{-1}): 3445 M $\nu(NH_2, NH)$; 1612 S $\nu(C{=}O)$, $\delta(NH_2)$, δ(NH, amide), 1480 w ν(CN, amide); 1220 e 1137 S ν(C–N); 909 w, 836 w, 765 w.

Synthesis of 2-amino-*N*-(6-((2-aminoethyl)(2-(3,5-dimethyl-1*H*-pyrazol-1-yl)ethyl)amino)-hexyl)-5-guanidinopentanamide (L^2)

Removal of the Boc protecting group of **L^2-Boc** was done following the methodology described for **L^1-Boc**. The residue obtained after evaporation of the solvents was dissolved in water, filtered through a 0.45 μm Millipore filter, and purified by preparative RP-HPLC. The fractions containing **L^2** were collected and the solvent was removed to provide a yellow viscous oil. Yield: 90.4% (0.019 g, 0.043 mmol, calcd for $C_{21}H_{43}N_9O$).

^{1}H-NMR (300 MHz, D_2O): δ_H (ppm) 6.02 (1H, s, H^b), 4.42 (2H, t, H^d), 3.83 (1H, t, H^n), 3.69 (2H, t, H^e), 3.51 (2H, m, H^f), 3.35 (2H, m, $H^{g',\ g''}$), 3.13 (6H, m, $H^{q,\ h,\ m}$), 2.21 (3H, t, CH_3^{Pz}), 2.13 (3H, s, CH_3^{Pz}), 1.78 (2H, m, H^o) 1.55–1.49 (4H, m, $H^{i,\ p}$), 1.42–1.32 (2H, m, H^l), 1.22 (4H, m, $H^{j,\ k}$).

^{13}C-NMR (75.5 MHz, D_2O): δ_C (ppm) 169.6 (CO), 156.8 (C^r), 148.2 (C^{Pz}), 145.8 (C^{Pz}), 107.9 (C^b), 53.9 (C^q), 52.9 (C^n), 51.0 (C^e), 49.7 (C^f), 42.0 (C^d), 40.3 (C^m), 39.4 (C^h), 33.6 (C^g), 28.0 ($C^{o,\ l}$), 25.6 (C^p), 25.2 (C^i), 23.7 (C^k), 22.8 (C^j), 10.9 (CH_3^{Pz}), 10.1 (CH_3^{Pz}).

RP-HPLC (t_R): 19.5 min.

ESI-MS (+) (m/z): 220 $[M + H]^{2+}$, 439 $[M + H]^+$, calcd for $C_{21}H_{43}N_9O$ = 438.

IR (KBr, cm^{-1}): 3312 M $\nu(NH_2, NH)$; 1671 S $\nu(C{=}O)$, $\delta(NH_2)$, δ(NH, amide), 1421 w ν(CN, amide); 1209 and 1190 S ν(C–N); 898 w, 823 w, 748 w.

General procedure for the preparation of the Re complexes *fac*-$[Re(CO)_3(k^3\text{-}L)]^+$ (Re1, L = L1; Re2, L = L2)

$[Re(CO)_3(H_2O)_3]Br$ was reacted with equimolar amounts of **L^1** or **L^2** in refluxing water for 12 h. The solvent was concentrated to $\frac{1}{4}$ of the volume and the resulting solution was centrifuged and the supernatant was purified by preparative RP-HPLC.

Synthesis of *fac*-$[Re(CO)_3(k^3\text{-}L^1)]^+$ (Re1). Starting from 0.020 g (0.048 mmol) of **L^1**, a colorless oil formulated as **Re1** was obtained. Yield: 33.3% (0.010 g, 0.014 mmol, calcd for $C_{22}H_{41}N_9O_4Re$).

^{1}H-NMR (300 MHz, D_2O): δ_H (ppm) 6.08 (1H, s, H^b), 5.10 (1H, s, NH), 4.35 (1H, dd, $H^{d'}$), 4.14–3.98 (1H, m, $H^{d''}$), 3.87 (1H, t, H^n), 3.71–3.66 (2H, m, NH), 3.59–3.50 (1H, m, $CH^{h'}$), 3.40–3.19 (4H, m, $H^{h'',\ e',\ j}{}_2$), 3.11 (3H, m, $H^{g',\ q}{}_2$), 2.75 (2H, m, H^f), 2.67–2.63 (1H, m, $H^{e''}$), 2.50–2.39 (1H, m, $H^{g''}$), 2.30 (3H, s, CH_3^{Pz}), 2.19 (3H, s, CH_3^{Pz}), 2.10–1.91 (1H, m, $H^{i'}$), 1.86–1.75 (3H, m, $H^{i'',\ o}{}_2$), 1.61–1.50 (2H, m, $H^p{}_2$).

^{13}C-NMR (75.5 MHz, D_2O): δ_C (ppm) 196.1, 194.9, 194.7 (CO, Re), 171.6 (C═O), 164.7 (C^r), 155.7 (C^{Pz}), 146.2 (C^{Pz}), 109.8 (C^{Pz}), 66.7 (C^h), 63.7 (C^f), 55.1 (C^n) 55.4 (C^e), 49.0 (C^d), 44.1 (C^g), 42.4 (C^j), 39.3 (C^q), 30.1 (C^o), 26.2 (C^i), 25.8 (C^p), 17.2 (CH_3^{Pz}), 12.8 (CH_3^{Pz}).

RP-HPLC (t_R): 25.1 min.

ESI-MS (+) (m/z): 342 $[M + 2H]^{2+}$, calcd for $C_{21}H_{37}N_9O_4Re$ = 681.3.

IR (KBr, cm^{-1}): 3276 M $\nu(NH_2$ NH); 2026, 1915 S (CO); 1676 S (C═O), $\delta(NH_2)$, 1208–1135 M ν(CN); 876 w; 758 w; 683 w.

Synthesis of *fac*-$[Re(CO)_3(k^3\text{-}L^2)]^+$ (Re2). Starting from 0.020 g (0.045 mmol) of **L^2**, a colorless oil formulated as **Re^2** was obtained. Yield: 37.5% (0.012 g, 0.017 mmol, calcd for $C_{24}H_{43}N_9O_4Re$).

^{1}H-NMR (300 MHz, D_2O): δ_H (ppm) 6.05 (1H, s, H^b), 5.04 (1H, s, NH), 4.32 (1H, dd, $H^{d'}$), 4.08 (1H, dd, $H^{d''}$), 3.82 (1H, t, H^n), 3.61 (2H, s, NH), 3.50–3.40 (1H, m, $H^{h'}$), 3.30–3.18 (3H, m, $H^{h'',\ m}{}_2$), 3.07 (3H, m, $H^{e',\ g',\ q}{}_2$), 2.70 (2H, m, $H^f{}_2$), 2.53 (1H, m, $H^{e''}$), 2.40 (1H, m, $H^{g''}$), 2.27 (3H, s, H^{Pz}), 2.16 (3H, s, H^{Pz}), 1.76 (3H, m, $H^{o',\ o'',\ i''}$), 1.69–1.58 (1H, m, $H^{i''}$), 1.49 (4H, m, $H^p{}_{2',\ l}{}_2$) 1.61–1.50 (2H, m, $H^j{}_{2',\ k}{}_2$).

^{13}C-NMR (75.5 MHz, D_2O): δ_C (ppm) 194.7, 194.4, 193.0 (CO, Re); 169.2 (C═O), 156.9 (C^r), 153.7 (C^{Pz}), 144.2 (C^{Pz}), 107.9 (C^{Pz}), 67.6 (C^h), 61.9 (C^f) 53.3 (C^e), 53.3 (C^n), 47.0 (C^d), 42.2 (C^g), 40.5 (C^m), 39.6 (C^q), 28.2 (C^l), 28.2 (C^o), 25.9 ($C^{j,\ K}$), 24.4 (C^i), 23.8 (C^l), 15.3 (CH_3^{Pz}), 10.9 (CH_3^{Pz}).

RP-HPLC (t_R): 25.5 min.

ESI-MS (+) (m/z): 355 $[M + 2H]^{2+}$, calcd for $C_{24}H_{43}N_9O_4Re$ = 708.

IR (KBr, cm^{-1}): 3274 M $\nu(NH_2$ NH); 2028, 1914 S (CO); 1675 S (C═O), $\delta(NH_2)$, 1206–1135 M ν(CN); 877 w; 760 w; 684 w.

General method for the synthesis of the ^{99m}Tc(I) complexes *fac*-$[^{99m}Tc(CO)_3(k^3\text{-}L)]^+$ (L = L^1 and L^2)

In a nitrogen-purged glass vial, 100 mL of a 10^{-4} M aqueous solution of compound **L1** or **L2** were added to 900 mL of a solution of the organometallic precursor *fac*-$[^{99m}Tc(CO)_3(H_2O)_3]^+$ (1–2 mCi) in saline or phosphate buffer pH 7.4. The reaction mixture was then heated to 100 °C for 30 min, cooled on an ice bath and the final solution was analyzed by RP-HPLC. Retention times: 25.9 min (**Tc1**), 26.6 min (**Tc2**). Complexes **Tc3–Tc5** were prepared and characterized as described previously.[22,28]

In vitro stability studies in plasma

100 μL of **Tc1** or **Tc2** were added to 500 μl of human plasma and incubated at 37 °C. After 24 h, aliquots (100 μL) were taken and the plasmatic proteins were precipitated with ethanol (200 μL). The plasma was centrifuged at 3000 rpm for 15 min at 4 °C and the supernatant (protein-free plasma) was filtered through a Millipore filter (0.22 μm), and analyzed by RP-HPLC.

Enzymatic assays

The iNOS activity assay was based on the method of hemoglobin assay previously described by Hevel and Marletta with slight modifications.[36,37] The kinetic parameters for iNOS were determined using initial rate analysis. Initial rate data were fitted to irreversible single substrate Michaelis–Menten models. The kinetic parameters were determined using the direct linear plot of Eisenthal and Cornish-Bowden and the Hyper software (J. S. Easterby, University of Liverpool, UK; http://www.liv.ac.uk/~jse/software.html).[38] This method was chosen primarily because of its robustness.[39] The K_m values represent a mean of triplicate measurements. Standard deviations of ±5 to 10% were observed.

Preparation of oxyhemoglobin

Oxyhemoglobin was prepared using a previously described protocol with some modifications.[40] Briefly, bovine hemoglobin in 50 mM HEPES pH 7.4 was reduced to oxyhemoglobin with 10-fold molar excess of sodium dithionite. The sodium dithionite was later removed by dialysis against 50 volumes of HEPES buffer for 18 h at 4 °C. The buffer was replaced 3 times. The concentration of oxyhemoglobin was determined spectrophotometrically using $\varepsilon_{415\ nm} = 131\ mM^{-1}\ cm^{-1}$. Oxyhemoglobin was stored at −80 °C before use.

Determination of K_m values

All initial velocity measurements were recorded at 37 °C. Total reaction volumes were 1500 μL and contained 50 mM HEPES pH 7.4, 6 mM oxyhemoglobin, 200 mM NADPH, 10 mM tetrahydrobiopterin (BH_4), 100 mM DTT and increasing concentrations of L-Arg, **L1**, **L2**, **Re1** and **Re2** (20–500 mM). Magnetic stirring in the spectrophotometer cuvette was essential to maintain isotropic conditions. Reactions were initiated by the addition of the iNOS enzyme (~1 U) to the pre-warmed cuvette (~5 min). The NO-mediated conversion of oxyhemoglobin to methemoglobin was followed by monitoring the increase in absorbance at dual wavelengths (401 and 421 nm) for 10 min.[41] Controls were performed under the same conditions without the iNOS enzyme.

Cell culture

RAW 264.7 macrophages, and the following human tumoral cell lines: HeLa cervical cancer, A375 melanoma, MDA-MB-231 breast cancer and PC3 prostate cancer, were grown in Dulbecco's Modified Eagle's Medium (DMEM) with GlutaMax I supplemented with 10% heat-inactivated fetal bovine serum (FBS) and 1% penicillin/streptomycin antibiotic solution (all from Invitrogen, UK). Cells were cultured under a humidified atmosphere of 95% air and 5% CO_2 at 37 °C, with the medium changed every other day.

Cellular uptake and internalization

Cellular uptake assays with **Tc1**–**Tc5** were performed in HeLa, A375, MDA-MB-231 and PC3 cell lines seeded at a density of 0.2 million cells per well in 24-well tissue culture plates. Cells were allowed to attach overnight. On the following day the cells were exposed to complexes (about 200 000 cpm in 0.5 mL of assay medium: Dulbecco's Modified Eagle's Medium with 25 mM HEPES and 0.2% BSA) for a period of 5 min to 4 h. Incubation was terminated by removing the Tc-complexes and by washing cells twice with ice-cold PBS with 0.2% BSA. Then, the cells were lysed by 10 min incubation with 1 M NaOH at 37 °C and the activities of the lysates were measured in a γ-counter. The percentage of cell-associated radioactivity was calculated and represented as a function of incubation time. Uptake studies were carried out using at least four replicates for each time point.

The cellular uptake of **Tc2** was also evaluated in the presence of *N*-ethylmaleimide (NEM), a specific inhibitor of system y^+. The cells were incubated with solutions of **Tc2** containing NEM (5 mM) for different periods (5, 15, 30 and 60 min) at 37 °C. The general procedure of cellular uptake was followed. The inhibition of cellular uptake was expressed in percentage of the uptake of **Tc2** in the absence of an inhibitor.

Internalization assays of the **Tc2** complex were performed in HeLa, A375 and MDA-MB-231 cell lines seeded at a density of 0.2 million cells per well in 24-well tissue culture plates. On the following day, the cells were exposed to **Tc2** (about 200 000 cpm in 0.5 mL of assay medium) for a period of 5 min to 4 h. Incubation was terminated by washing the cells with ice-cold assay medium. Cell surface-bound **Tc2** was removed by two steps of acid wash (50 mM glycine·HCl/100 mM NaCl, pH 2.8) at room temperature for 4 min. The pH was neutralized with cold PBS with 0.2% BSA. The cells were then lysed by 10 min incubation with 0.5 N NaOH at 37 °C to determine internalized **Tc2**. The activities of the lysates and cell surface-bound fractions were measured in a γ-counter.

Internalization assays for **Tc2** were also performed in the presence of L-lysine. For this study, A375, HeLa and MDA-231 cells were incubated 2 h at 37 °C with solutions of **Tc2** containing different concentrations of L-lysine (0, 0.5, 1, 5 and 10 mM).

Cell viability determination

Cell viability was evaluated by using a colorimetric method based on the tetrazolium salt [3-(4,5-dimethylthiazol-2-yl)-2,5-diphenyltetrazolium bromide (MTT), which is reduced by viable cells to yield purple formazan crystals.[42] RAW 264.7 macrophages in DMEM medium without arginine supplemented with 10% FBS were seeded in 96-well plates at a density of 9×10^4 cells per well, immediately induced with LPS (2 mg mL^{-1}) for 4 h, and then incubated for 24 h in the presence of the compounds (500 μM) and arginine (when indicated).[22] At the end of the incubation period the media were removed and the cells were incubated with MTT (0.5 mg mL^{-1} in culture medium; 200 mL) for 3–4 h at 37 °C and 5% CO_2. The purple formazan crystals formed inside the cells were then dissolved in 200 mL of DMSO by thorough shaking, and the absorbance was read at 570 nm, using a plate spectrophotometer (Power Wave Xs; Bio-Tek). Each test was performed with at least six replicates and repeated at least 2 times. The

result was expressed as a percentage of the surviving cells in relation to the control.

Assay of iNOS activity *in vivo*

RAW 264.7 macrophages in DMEM medium without arginine supplemented with 10% FBS DMEM were plated at a density of 9×10^4 cells per well in 96-well plates. The cells were immediately induced with 10 μL of LPS (2 μg mL^{-1} in PBS) for 4 h, and then incubated for 24 h in the presence of the compounds (500 μM). At the end of the incubation period, the culture medium was collected and assayed for nitrite production using the commercially available Griess reagent (1% sulfanilamide, 0.1% *N*-1-naphthyl ethylenediamine, 2.5% orthophosphoric acid; Sigma-Aldrich). Briefly, 50 μL of Griess reagent was mixed with an equal volume of medium at room temperature and the absorbance was measured at 540 nm after 10 min. Fresh culture medium served as the blank in all experiments. Each experiment was performed with six replicates and repeated three times.

Western blot

Western blot experiments were performed to demonstrate the expression of CAT-1 in the four human tumoral cell lines (A375, HeLa, MDA-MB-231 and PC3). The cells were lysed with the CelLytic™ M Extraction Reagent (Sigma) supplemented with Complete Protease Inhibitor Cocktail tablets (Roche). After 15 min at 4 °C with regular shaking, lysates were collected and centrifuged at 14 000*g* for 10 min to pellet the cellular debris, and the supernatants were removed for further use. The total protein content was determined using the DC Protein Assay Kit (BioRad). Samples (50 μg of protein) were separated by sodium dodecyl sulfate-polyacrylamide gel electrophoresis (SDS-PAGE) and transferred onto nitrocellulose membranes. Blots were blocked with 5% nonfat dry milk in PBS-T for 2 h and then incubated for 1 h with the primary antibodies against CAT-1 (1 : 200, Santa Cruz, sc-66824) and actin (1 : 15 000, Sigma, A3853). Membranes were washed with PBS-T and incubated for 1 h with the secondary antibodies in a 1 : 3000 dilution (goat anti-rabbit IgG-HRP for α-CAT-1 and goat anti-mouse IgG-HRP for α-actin, BioRad). Membranes were developed using the SuperSignal West Pico Substrate kit (Pierce, Rockford, IL) according to the manufacturer's instructions.

Author contributions

J. D. G. C. and B. L. O. conceived the experimental strategy; F. F. and M. M. performed the synthesis, radiolabelling and enzymatic studies; V. F. C. F. conducted cell culture, internalization studies and western blotting; P. R. and F. M. provided intellectual input on the cellular studies, enzymatic studies in cells and western blotting; I. S., B. L. O and J. D. G. C. prepared the draft and final version of the manuscript. B. L. O. and J. D. G. C. are co-senior authors of this work.

Acknowledgements

This work has been partially supported by the Fundação para a Ciência e Tecnologia (FCT), Portugal, through the UID/Multi/04349/2013 project. V. F. C. F. thanks FCT for a PhD grant (SFRH/BD/108623/2015). Dr J. Marçalo is acknowledged for performing the ESI-MS analyses. The QITMS instrument was acquired with the support of Contract REDE/1503/REM/2005 – ITN of FCT and is part of RNEM.

References

1 S. L. Pimlott and A. Sutherland, *Chem. Soc. Rev.*, 2011, **40**, 149–162.
2 S. N. Histed, M. L. Lindenberg, E. Mena, B. Turkbey, P. L. Choyke and K. A. Kurdziel, *Nucl. Med. Commun.*, 2012, **33**, 349–361.
3 H. Schoder and S. M. Larson, *Semin. Nucl. Med.*, 2004, **34**, 274–292.
4 A. Sundin, U. Garske and H. Orlefors, *Best Pract. Res., Clin. Endocrinol. Metab.*, 2007, **21**, 69–85.
5 J. McConathy and M. M. Goodman, *Cancer Metastasis Rev.*, 2008, **27**, 555–573.
6 J. McConathy, W. Yu, N. Jarkas, W. Seo, D. M. Schuster and M. M. Goodman, *Med. Res. Rev.*, 2012, **32**, 868–905.
7 R. Hyde, P. M. Taylor and H. S. Hundal, *Biochem. J.*, 2003, **373**, 1–18.
8 E. I. Closs, J. P. Boissel, A. Habermeier and A. Rotmann, *J. Membr. Biol.*, 2006, **213**, 67–77.
9 C. Huang and J. McConathy, *J. Nucl. Med.*, 2013, **54**, 1007–1010.
10 K. K. S. Sai, C. Huang, L. Yuan, D. Zhou, D. Piwnica-Worms, J. R. Garbow, J. A. Engelbach, R. Mach, K. M. Rich and J. McConathy, *J. Nucl. Med.*, 2013, **54**, 1120–1126.
11 E. I. Closs, A. Simon, N. Vekony and A. Rotmann, *J. Nutr.*, 2004, **134**, 2752S–2759S.
12 S. Moncada, R. M. J. Palmer and E. A. Higgs, *Pharmacol. Rev.*, 1991, **43**, 109–142.
13 D. Fukumura, S. Kashiwagi and R. K. Jain, *Nat. Rev. Cancer*, 2006, **6**, 521–534.
14 P. Mukherjee, M. A. Cinelli, S. Kang and R. B. Silverman, *Chem. Soc. Rev.*, 2014, **43**, 6814–6838.
15 M. M. Phillips, M. T. Sheaff and P. W. Szlosarek, *Cancer Res. Treat.*, 2013, **45**, 251–262.
16 N. Gupta, S. Miyauchi, R. G. Martindale, A. V. Herdman, R. Podolsky, K. Miyake, S. Mager, P. D. Prasad, M. E. Ganapathy and V. Ganapathy, *Biochim. Biophys. Acta*, 2005, **1741**, 215–223.
17 N. Gupta, P. D. Prasad, S. Ghamande, P. Moore-Martin, A. V. Herdman, R. G. Martindale, R. Podolsky, S. Mager, M. E. Ganapathy and V. Ganapathy, *Gynecol. Oncol.*, 2006, **100**, 8–13.
18 S. Karunakaran, S. Ramachandran, V. Coothankandaswamy, S. Elangovan, E. Babu, S. Periyasamy-Thandavan, A. Gurav,

J. P. Gnanaprakasam, N. Singh, P. V. Schoenlein, P. D. Prasad, M. Thangaraju and V. Ganapathy, *J. Biol. Chem.*, 2011, **286**, 31830–31838.
19 Y. Lu, W. Wang, J. Wang, C. Yang, H. Mao, X. Fu, Y. Wu, J. Cai, J. Han, Z. Xu, Z. Zhuang, Z. Liu, H. Hu and B. Chen, *PLoS One*, 2013, **8**, e73866.
20 S. A. Abdelmagid, J. A. Rickard, W. J. McDonald, L. N. Thomas and C. K. L. Too, *J. Cell. Biochem.*, 2011, **112**, 1084–1092.
21 Y. Liu, J. K. Pak, P. Schmutz, M. Bauwens, J. Mertens, H. Knight and R. Alberto, *J. Am. Chem. Soc.*, 2006, **128**, 15996–15997.
22 B. L. Oliveira, P. D. Raposinho, F. Mendes, F. Figueira, I. Santos, A. Ferreira, C. Cordeiro, A. P. Freire and J. D. G. Correia, *Bioconjugate Chem.*, 2010, **21**, 2168–2172.
23 A. de Almeida, B. L. Oliveira, J. D. G. Correia, G. Soveral and A. Casini, *Coord. Chem. Rev.*, 2013, **257**, 2689–2704.
24 B. L. Oliveira, I. S. Moreira, P. A. Fernandes, M. J. Ramos, I. Santos and J. D. G. Correia, *J. Mol. Model.*, 2013, **19**, 1537–1551.
25 B. L. Oliveira, I. S. Moreira, P. A. Fernandes, M. J. Ramos, I. Santos and J. o. D. G. Correia, *J. Mol. Graphics Modell.*, 2013, **45**, 13–25.
26 B. L. Oliveira, M. Morais, F. Mendes, I. S. Moreira, C. Cordeiro, P. A. Fernandes, M. J. Ramos, R. Alberto, I. Santos and J. D. G. Correia, *Chem. Biol. Drug Des.*, 2015, **86**, 1072–1086.
27 M. Morais, A. Paulo, L. Gano, I. Santos and J. D. G. Correia, *J. Organomet. Chem.*, 2013, **744**, 125–139.
28 B. L. Oliveira, J. D. G. Correia, P. D. Raposinho, I. Santos, A. Ferreira, C. Cordeiro and A. P. Freire, *Dalton Trans.*, 2009, 152–162.
29 B. L. Oliveira, J. D. G. Correia, P. D. Raposinho, I. Santos, A. Ferreira, C. Cordeiro and A. P. Freire, *Dalton Trans.*, 2009, 152–162.
30 M. Pan, H. A. Choudry, M. J. Epler, Q. H. Meng, A. Karinch, C. M. Lin and W. Souba, *J. Nutr.*, 2004, **134**, 2826S–2829S.
31 D. Fotiadis, Y. Kanai and M. Palacin, *Mol. Aspects Med.*, 2013, **34**, 139–158.
32 C. Fleck, M. Schwertfeger and P. M. Taylor, *Amino Acids*, 2003, **24**, 347–374.
33 S. R. Beyer, R. T. Mallmann, I. Jaenecke, A. Habermeier, J. P. Boissel and E. I. Closs, *J. Biol. Chem.*, 2013, **288**, 30411–30419.
34 J. MacMicking, Q. W. Xie and C. Nathan, *Annu. Rev. Immunol.*, 1997, **15**, 323–350.
35 N. Lazarova, S. James, J. Babich and J. Zubieta, *Inorg. Chem. Commun.*, 2004, **7**, 1023–1026.
36 J. Hevel and M. Marletta, *Methods Enzymol.*, 1994, **233**, 250–258.
37 S. Archer, *FASEB J.*, 1993, **7**, 349–360.
38 R. Eisenthal and A. Cornish-Bowden, *Biochem. J.*, 1974, **139**, 715–720.
39 A. Cornish-Bowden, *Fundamentals of Enzyme Kinetics*, Portland Press, London, 2nd edn, 1995.
40 D. J. Wolff, D. S. Gauld, M. J. Neulander and G. Southan, *J. Pharmacol. Exp. Ther.*, 1997, **283**, 265–273.
41 R. G. Knowles and S. Moncada, *Biochem. J.*, 1994, **298**, 249–258.
42 T. Mosmann, *J. Immunol. Methods*, 1983, **65**, 55–63.